# Threoninol as a scaffold of dyes (threoninol-nucleotide) and their stable interstrand clustering in duplexes†

**Hiromu Kashida,[a] Taiga Fujii[a] and Hiroyuki Asanuma*[a,b]**

***Received 15th April 2008, Accepted 16th May 2008***
***First published as an Advance Article on the web 13th June 2008***
**DOI: 10.1039/b806406g**

Functional molecules such as dyes (Methyl Red, azobenzene, and Naphthyl Red) were tethered on D-threoninol as base surrogates (threoninol-nucleotide), which were consecutively incorporated at the center of natural oligodeoxyribonucleotides (ODNs). Hybridization of two ODNs involving threoninol-nucleotides allowed interstrand clustering of the dyes on D-threoninol and greatly stabilized the duplex. When two complementary ODNs, both of which had tethered Methyl Reds on consecutive D-threoninols, were hybridized, the melting temperature increased proportionally to the number of Methyl Reds, due to stacking interactions. Clustering of Methyl Reds induced both hypsochromicity and narrowing of the band, demonstrating that Methyl Reds were axially stacked relative to each other (H-aggregation). Since hybridization lowered the intensity of circular dichroism peaks at the π–π* transition region of Methyl Red (300–500 nm), clustered Methyl Reds were scarcely wound in the duplex. Alternate hetero dye clusters could also be prepared only by hybridization of two ODNs with different threoninol-nucleotides, such as Methyl Red–azobenzene and Methyl Red–Naphthyl Red combinations. A combination of Methyl Red and azobenzene induced bathochromic shift and broadening of the band at the Methyl Red region due to the disturbance of exciton interaction among Methyl Reds. But interestingly, the Methyl Red and Naphthyl Red combination induced merging of each absorption band to give a single sharp band, indicating that exciton interaction occurred among the different dyes. Thus, D-threoninol can be a versatile scaffold for introducing functional molecules into DNA for their ordered clustering.

## Introduction

Modification of nucleotides is one of the most active research fields in chemical biology. A wide variety of modified oligodeoxyribonucleotides (ODNs) have been synthesized for reasons such as expansion of the genetic alphabet,[1] antigene or antisense therapy,[2] and fluorescent labeling.[3] Moreover, ODNs have been also utilized as a scaffold for preparing supramolecular arrays.[4–6] For example, Tanaka and Shionoya *et al*. reported on metal arrays of copper(II) ions in an ODN double helix by introducing metal ligands into the base positions.[4] Kool *et al.* reported on arrays of fluorescence dyes, made by consecutively introducing dyes into a single strand.[5] They succeeded in constructing arrays of functional molecules of pre-determined size and number. In these reports, metal ligands or fluorescent dyes were introduced at the C1′ position of D-ribose as non-natural bases.

One of the reasons for utilizing D-ribose is that functional molecules can be incorporated into natural ODNs without distorting their natural B-type structure. Furthermore, functional molecules on natural nucleotides can be substrates of DNA or RNA polymerase, and in some cases can be enzymatically incorporated into ODNs.[7] This latter purpose inevitably requires the natural D-ribose backbone. However, there is no limitation on the structure of a scaffold when the ODNs are designed for use as supramolecular material scaffolds and are not enzymatically but chemically synthesized. Non-natural scaffolds should extend the variety of ODNs and their helical structure, and will lead to new functional supramolecular helices without the assistance (and limitations) of natural nucleotides. Although many non-natural scaffolds have been proposed so far,[8] most of them were aimed at tethering natural nucleobases (such as thymine and adenine) and were mainly focused on resistance to enzymatic breakdown for use in antisense strand gene therapies. Thus, only a limited number have been reported on *non-natural* and chiral scaffolds for tethering *non-natural* functional molecules.[9]

Threoninol is an amino acid derivative that can be synthesized by one-step reduction from threonine.[10] Previously, we have synthesized modified ODNs incorporating D-threoninol (not the L-form) as a linker,[11] and found that even non-natural molecules on this linker intercalated between base pairs without destabilizing the duplex. Here, we propose D-threoninol as a useful scaffold (threoninol-nucleotide) of various non-natural functional molecules for incorporating them into ODNs and tethering

[a]*Graduate School of Engineering, Nagoya University, Furocho, Chikusa, Nagoya, 464-8603, Japan. E-mail: asanuma@mol.nagoya-u.ac.jp; Fax: +81-52-789-2528; Tel: +81-52-789-2488*
[b]*Core Research for Evolution Science and Technology (CREST), Japan Science and Technology Agency (JST), Kawaguchi, Saitama, 332-0012, Japan*

† Electronic supplementary information (ESI) available: UV–Vis spectra of single-stranded **M1b**, **Z3a**–**M3b** and Methyl Red–Naphthyl Red hetero aggregates containing spacers; tables listing melting temperatures, absorption maxima and half-line widths of **A*n*a**–**M*n*b** duplexes. See DOI: 10.1039/b806406g

 

various dyes on to it, without disturbing hybridization to a complementary ODN. In our design, non-natural functional molecules on D-threoninol (threoninol-nucleosides) are introduced at the counterpart of each strand to form a pseudo "base-pair". Larger molecules than natural bases can be introduced and pseudo "base-pairs" stabilize the duplex by intermolecular stacking interactions as depicted in Scheme 1. By this design, highly organized molecular clusters can be easily constructed without disturbing the duplex. Such molecular clusters are applicable to nonlinear optical materials and molecular wire as well as detection of single nucleotide polymorphisms and so on. Recently, Brotschi *et al.* reported zipper-like DNA that tethered aromatic non-natural bases on D-ribose, and the duplex was stabilized by interstrand stacking of the incorporated molecules.[12] We use D-threoninol instead of D-ribose as a scaffold and expect interstrand anti-parallel stacking with a larger cross-section area due to the flexibility of threoninol.

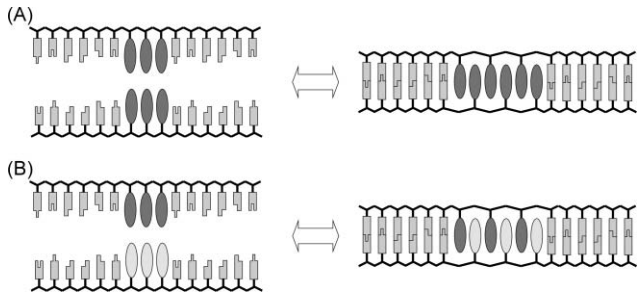


**Scheme 1** Schematic illustration of stabilization by insertion of threoninol-nucleotides of (A) homo and (B) hetero pairs.

In the present study, three threoninol-nucleotides tethering Methyl Red (**M**), Naphthyl Red (**N**) and azobenzene (**Z**) were prepared and incorporated into ODNs (Scheme 1). Interstrand stacking of these dyes was investigated from UV–Vis and CD spectra as well as the melting profiles of the resulting duplexes. We found that D-threoninol could be a useful scaffold of non-natural molecules, for their clustering in the duplex and stabilization of the duplex. By these threoninol-nucleotides, homo- and alternate hetero-clusters can be easily designed and synthesized.

## Results

### 1. Effect of the pairing of threoninol-nucleotides on the melting temperature

**Homo-combination.** The sequences of the ODNs involving threoninol-nucleotides are shown in Scheme 2: threoninol-nucleotides (**M**, **N**, and **Z** in Scheme 2) were introduced consecutively into the middle of ODNs. Here, they are located at the counterpart of each strand to form a pseudo "base-pair" with an anti-parallel orientation (see Scheme 1). First, the effect of pairing of threoninol-nucleotides on the stability of the duplex (melting temperature, $T_m$) was examined. Fig. 1A shows $T_m$s of **M*n*a/M*n*b** (circles), **Z*n*a/Z*n*b** (triangles), and **M*n*a/Z*n*b** (squares) determined from the change of absorbance at 260 nm. When **M1a** and **M1b**, both of which involve single threoninol-nucleotide of Methyl Red (**M** residue), were hybridized, its $T_m$ was determined as 50.5 °C as listed in Table 1 (and also plotted in Fig. 1A), which

**M*n*a** : 5'-GGT-ATC-**M**$_n$-GCA-ATC-3' ***n*** = 1-6
**M*n*b** : 3'-CCA-TAG-**M**$_n$-CGT-TAG-5'

**Z*n*a** : 5'-GGT-ATC-**Z**$_n$-GCA-ATC-3' ***n*** = 1,2,3,6
**Z*n*b** : 3'-CCA-TAG-**Z**$_n$-CGT-TAG-5'

**MS3a**: 5'-GGT-ATC-**MSMSMS**-GCA-ATC-3'
**MS3b**: 3'-CCA-TAG-**SMSMSM**-CGT-TAG-5'

**N3a** : 5'-GGT-ATC-**N**$_3$-GCA-ATC-3'
**A*n*a** : 5'-GGT-ATC-A$_n$-GCA-ATC-3' ***n*** = 1-6
**T5a** : 5'-GGT-ATC-T$_5$-GCA-ATC-3'
**C5a** : 5'-GGT-ATC-C$_5$-GCA-ATC-3'
**G5a** : 5'-GGT-ATC-G$_5$-GCA-ATC-3'

**N** : 5'-GGT-ATC-GCA-ATC-3'
**C** : 3'-CCA-TAG-CGT-TAG-5'

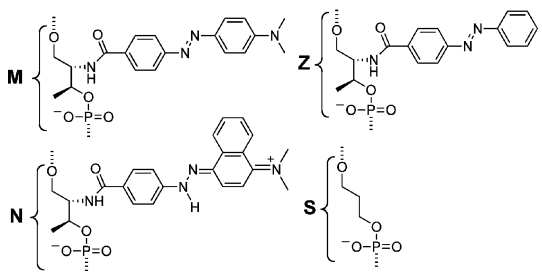


**Scheme 2** Sequences of ODNs synthesized in this study.

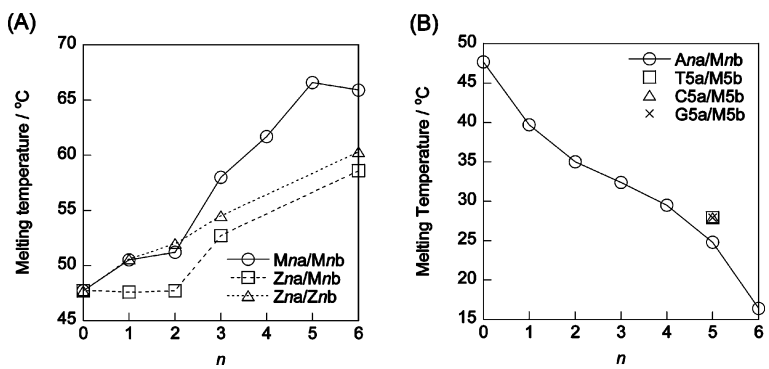


**Fig. 1** Melting temperatures of (A) threoninol-nucleotide pairs of **M*n*a**–**M*n*b** and **Z*n*a**–**Z*n*b** involving Methyl Red and azobenzene homo clusters, respectively, and **Z*n*a**–**M*n*b** involving an azobenzene–Methyl Red hetero cluster, (B) a natural and threoninol-nucleotide pair, **A*n*a**–**M*n*b**, involving adenosine and Methyl Red. Melting temperatures of **T5a**–**M5b**, **C5a**–**M5b**, and **G5a**–**M5b** are also shown. Melting temperatures of each duplex are listed in the ESI.† Solution conditions are as follows: [ODN] = 5 μM, [NaCl] = 100 mM, pH 7.0 (10 mM phosphate buffer).

**Table 1** Effects of the number of Methyl Red on the melting temperature ($T_m$) and absorption maximum and half-line-width of π–π* transition of Methyl Red[a]

| Sequences | $T_m$/°C | $\lambda_{max}$/nm[b] | Half-line width[b]/cm$^{-1}$ |
|---|---|---|---|
| **N–C** | 47.7 | — | — |
| **M1a–M1b** | 50.5 | 471 | 2883 |
| **M2a–M2b** | 51.2 | 446 | 3113 |
| **M3a–M3b** | 58.0 | 437 | 3112 |
| **M4a–M4b** | 61.7 | 429 | 3389 |
| **M5a–M5b** | 66.6 | 409 | 3228 |
| **M6a–M6b** | 65.9 | 404 | 2639 |
| **MS3a–MS3b** | 50.9 | 444 | 4543 |

[a] Solution conditions: [ODN] = 5 μM, [NaCl] = 100 mM, pH 7.0 (10 mM phosphate buffer). [b] UV–Vis spectrum was measured at 0 °C.

**Table 2** Melting temperatures of azobenzene–Methyl Red hetero- and azobenzene homo-cluster[a]

| | $T_m$/°C | |
|---|---|---|
| *n* | **Z*n*a–M*n*b** | **Z*n*a–Z*n*b** |
| 1 | 47.6 | 50.6 |
| 2 | 47.7 | 52.0 |
| 3 | 52.7 | 54.5 |
| 6 | 58.6 | 60.3 |

[a] Solution conditions: [ODN] = 5 μM, [NaCl] = 100 mM, pH 7.0 (10 mM phosphate buffer).

was 2.8 °C higher than that of the native **N–C** duplex (47.7 °C). The $T_m$ increased almost linearly as the number of **M** residues (*n*) increased from 1 to 5 and reached a plateau above $n \geq 5$ (see circles in Fig. 1A). Up to $n = 5$, the rate of $T_m$ increase was 3.6–3.7 °C per **M–M** pair. Thus, pairing of threoninol-nucleotides significantly stabilized the duplex. Similarly, the **Z*n*a–Z*n*b** combination involving azobenzene instead of Methyl Red also raised the $T_m$ almost linearly as the dye number increased to $n = 6$ (see Table 2 and triangles in Fig. 1A), although the $T_m$ increase was smaller (around 2.0 °C per **Z–Z** pair) than that of the **M–M** pair.

**Hetero-combinations of Z*n*a–M*n*b.** Hetero clusters were also easily prepared from the two ODNs, each of which had different threoninol-nucleotides. However, the hetero-combination **Z*n*a–M*n*b** was less stable in the duplex than the homo-combination (**M–M** or **Z–Z**). As summarized in Table 2, the $T_m$s of **Z1a–M1b** and **Z2a–M2b** were 47.6 and 47.7 °C, respectively, which were almost the same as that of the native **N–C** duplex, and were even lower than the $T_m$s of corresponding homo-combinations. In the cases of **Z3a–M3b** and **Z6a–M6b**, the $T_m$s were fairly high, although they were still lower than those of homo-combinations. The order of stability was **M–M** > **Z–Z** > **Z–M**, indicating that threoninol-nucleotides recognized themselves.

**Hetero-combinations of natural nucleotides and M*n*b.** In order to examine the possibility of clustering of threoninol-nucleotides with natural ones (A, T, G, and C), **M*n*b** was hybridized with natural ODN **A*n*a** involving an adenosine oligomer at its center. But unlike the threoninol-nucleotide pairs, the **A*n*a–M*n*b** combination uniformly decreased in $T_m$ with an increase in the number of adenosines (*n*), and the $T_m$ of the **A5a–M5b** duplex became as low as 24.8 °C, which was 23 °C lower than the native **N–C**, as shown in Fig. 1B.[13] Similarly, a combination of threoninol-nucleotide with other natural ones, thymidine, cytidine, and guanosine (**T5a–M5b**, **C5a–M5b**, and **G5a–M5b**) also drastically lowered the $T_m$. Thus, threoninol-nucleotides did not recognize natural nucleotides.

## 2. Spectroscopic behavior of the clustering of Methyl Reds

Most of the dyes exhibit distinct spectral changes upon clustering. Fig. 2A shows the effect of the temperature on the absorption spectrum of the **M3a–M3b** duplex. When the temperature was higher than 60 °C, where the duplex was dissociated, the solution gave an absorption maximum at 432 nm with a relatively broad peak (both $\lambda_{max}$ and half-line width of **M*n*a–M*n*b** duplex are summarized in Table 1). However, the spectrum became much narrower upon lowering the temperature below 40 °C (compare dotted line with solid line in Fig. 2A). As shown in Fig. 3, the melting profiles of **M3a–M3b** monitored at 260 nm (solid line) and 420 nm (dotted line), which were derived from the π–π* transition of Methyl Red moieties, were fairly synchronized. The $T_m$ determined from 260 nm was 58.0 °C, which almost coincided with that at 420 nm (56.6 °C). Furthermore, a simple sum of the absorption spectra of single-stranded **M3a** and **M3b** at 0 °C was obviously different from the spectrum of the **M3a–M3b** duplex as shown in Fig. 4: the **M3a–M3b** duplex (solid line in Fig. 4) showed narrowing as well as hypsochromicity in its absorption spectrum compared with their simple sum (dotted line). Thus, we could

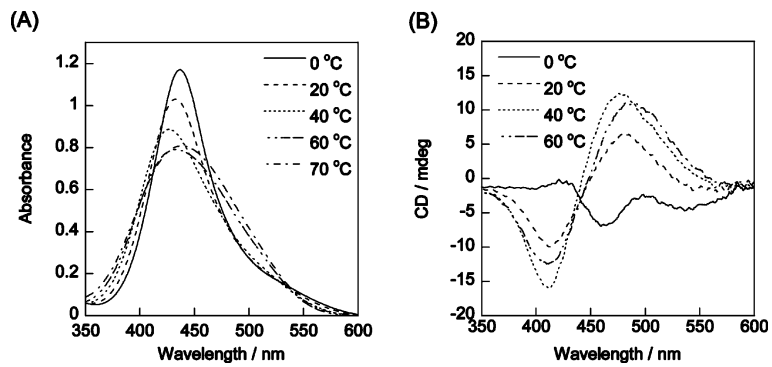


**Fig. 2** (A) UV–Vis and (B) CD spectra of **M3a–M3b** at various temperatures. Solution conditions are as follows: [ODN] = 5 μM, [NaCl] = 100 mM, pH 7.0 (10 mM phosphate buffer).

 

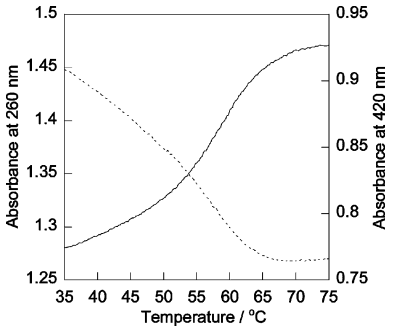


**Fig. 3** Melting curves of **M3a**–**M3b** monitored at 260 nm (solid line) and 420 nm (dotted line). Solution conditions are as follows: [ODN] = 5 μM, [NaCl] = 100 mM, pH 7.0 (10 mM phosphate buffer).

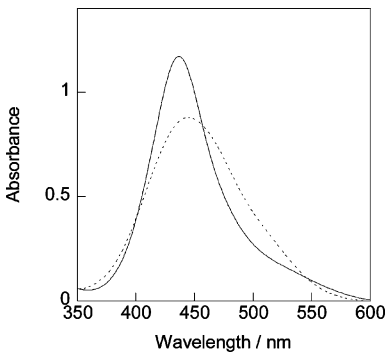


**Fig. 4** UV–Vis spectra of **M3a**–**M3b** duplex (solid line) and simple sum of the spectra of their single strands (dotted line) at 0 °C. Solution conditions are as follows: [ODN] = 5 μM, [NaCl] = 100 mM, pH 7.0 (10 mM phosphate buffer).

conclude that narrowing of the band was mostly attributed to the clustering of **M** residues, not to the simple temperature effect.

Clustering also affected circular dichroism (CD) spectra as depicted in Fig. 2B. At 60 °C, the solution of **M3a**–**M3b** displayed a relatively strong positive–negative Cotton effect at the π–π* transition region of Methyl Red, due to intrastrand exciton coupling of the chromophore in the single-stranded state (note that single-stranded **M3a** and **M3b** are chiral). However, CD was not enhanced at all by lowering the temperature. Rather, it became smaller at 0 °C where the cluster was firmly formed.

The number of pairs greatly affected the UV–Vis and CD spectra as shown in Fig. 5. The absorption maximum of the **M1a**–**M1b** duplex involving two Methyl Reds appeared at 471 nm at 0 °C, and an increase in the number of dyes induced continuous hypsochromic shift: $\lambda_{max}$ of **M2a**–**M2b**, **M3a**–**M3b**, and **M4a**–**M4b** were observed at 446, 437, and 429 nm, respectively (see Table 1). This hypsochromicity is characteristic of the so-called H-aggregates (H*-aggregates) in which chromophores are vertically stacked, and increases with the number of chromophores due to the extended exciton interaction.[14] The absorption maximum tended to converge at around 420 nm as deduced from the hypsochromic shift from **M3a**–**M3b** to **M4a**–**M4b**, which was only 8 nm. However, there was a small gap between **M4a**–**M4b** and **M5a**–**M5b**. **M5a**–**M5b** gave $\lambda_{max}$ at 409 nm, which was 20 nm shorter than that of **M4a**–**M4b**. In addition, significant narrowing of the band was induced with this increment (3228 and 2639 $cm^{-1}$ for **M5a**–**M5b** and **M6a**–**M6b**, respectively). Such a gap was also observed in the CD spectra. As shown in Fig. 5B, induced CD (ICD) was rather small in spite of the clustering of Methyl Reds when *n* in **M*n*A–M*n*B** was four and below. But a fairly strong ICD was observed for both **M5a**–**M5b** and **M6a**–**M6b** duplexes. These spectroscopic differences indicate that the stacked structures in **M5a**–**M5b** and **M6a**–**M6b** were different from other **M*n*A**–**M*n*B** ($n \leq 4$).

## 3. Insertion of spacer at the counterpart of threoninol-nucleotide

Previously, we have reported another type of pairing:[15] threoninol-nucleotide (**M** residue) and 1,3-propanediol (**S** in Scheme 2) were alternately incorporated, and **S** was located as the counterpart of **M** to form a tentative **M**–**S** pair, such as **MS3a**–**MS3b** in Scheme 2. In this **MS3a**–**MS3b** duplex, threoninol-nucleotides and spacer residues were introduced alternately into DNA and formed tentative **M**–**S** "base pairs". Although this design also allowed Methyl Reds to stack in an anti-parallel orientation, both the stability of the duplex and spectroscopic behavior were different. As listed in Table 1, the $T_m$ of **MS3a**–**MS3b** was 50.9 °C,[15a] which was about 3 °C higher than the native **N**–**C** duplex, but 7 °C lower than **M3a**–**M3b**. UV–Vis spectra of **M3a**–**M3b** and **MS3a**–**MS3b** are depicted in Fig. 6A. Although both duplexes contained six **M** residues, **M3a**–**M3b** exhibited a larger hypsochromic shift than **MS3a**–**MS3b** (compare **M3a**–**M3b** with **MS3a**–**MS3b** in Table 1). Furthermore, the spectrum of **M3a**–**M3b** was much narrower. These facts indicate stronger exciton interactions among the chromophores in **M3a**–**M3b** than in **MS3a**–**MS3b**. However,

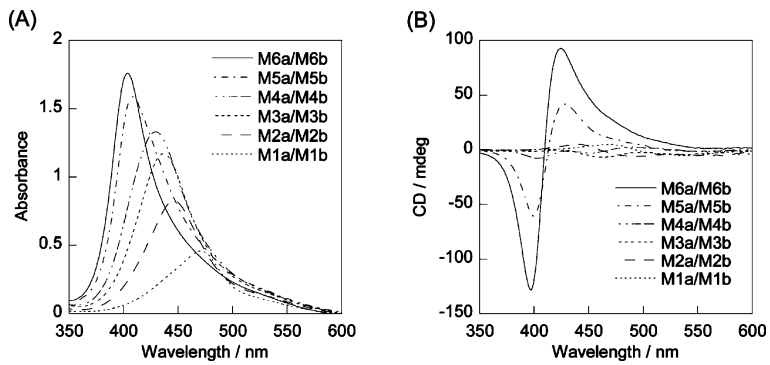


**Fig. 5** (A) UV–Vis and (B) CD spectra of the **M*n*a**–**M*n*b** ($1 \leq n \leq 6$) duplex at 0 °C. Solution conditions are as follows: [ODN] = 5 μM, [NaCl] = 100 mM, pH 7.0 (10 mM phosphate buffer).

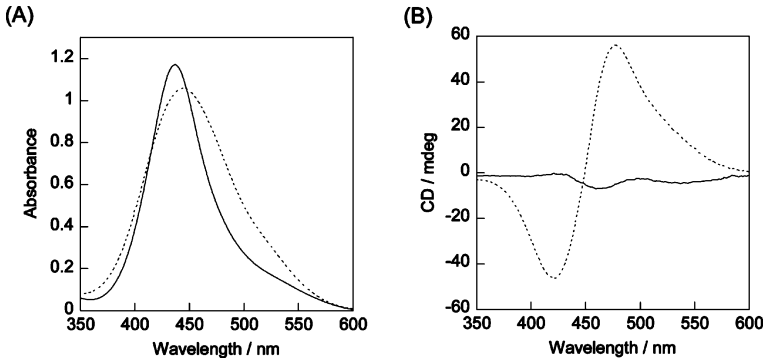


**Fig. 6** (A) UV–Vis and (B) CD spectra of **M3a**–**M3b** (solid line) and **MS3a**–**MS3b** (dotted line) at 0 °C. Solution conditions are as follows: [ODN] = 5 μM, [NaCl] = 100 mM, pH 7.0 (10 mM phosphate buffer).

the CD signal of **MS3a**–**MS3b** showed a much stronger positive and negative Cotton effect than that of **M3a**–**M3b** in spite of weaker exciton interaction (compare dotted line with solid line Fig. 6B).

## 4. Effect of hetero-combinations on the spectroscopic behavior

**Z6a–M6b combination.** As described above, hetero-combinations such as **Z*n*a–M*n*b** could also form relatively stable duplexes. In the case of a **M*n*a–M*n*b** homo-combination, clustering induced both narrowing and hypsochromicity due to the extended exciton interaction. In contrast, the **Z*n*a–M*n*b** combination induced bathochromic shift as well as broadening of the band at the π–π* region of Methyl Red. Fig. 7 shows the UV–Vis spectrum of the **Z6a**–**M6b** duplex as well as single-stranded **Z6a** and **M6b** under the same buffer conditions. **M6b** in the absence of **Z6a** gave $\lambda_{max}$ at 415 nm with a half-line width of 3662 $cm^{-1}$ as shown by the broken line in Fig. 7. Since **M1b** involving a single Methyl Red had $\lambda_{max}$ at 481 nm (see Fig. S-1 in the ESI†), Methyl Red chromophores in **M6b** excitonically interacted in the single-stranded state.[16] By hybridization with **Z6a**, however, $\lambda_{max}$ shifted to 429 nm with a half-line width of 4169 $cm^{-1}$. This bathochromicity and peak broadening demonstrated that Methyl Red and azobenzene moieties stacked alternately and intramolecular stacking among Methyl Reds in the single strand was weakened by azobenzene moieties. Similar broadening was also observed with **Z3a**–**M3b** (see Fig. S-2 in the ESI†).

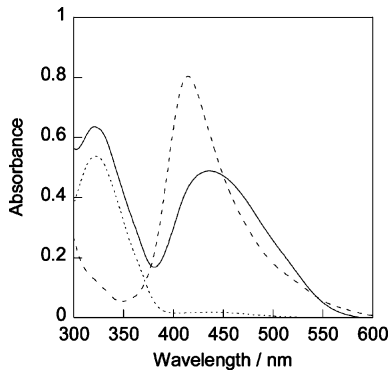


**Fig. 7** UV–Vis spectra of a hetero-cluster of Methyl Red and azobenzene (**Z6a**–**M6b**; solid line), single-stranded **Z6a** (dotted line) and **M6b** (broken line) at 0 °C. Solution conditions are as follows: [ODN] = 5 μM, [NaCl] = 100 mM, pH 7.0 (10 mM phosphate buffer).

**N3a–M3b combination.** Single-stranded **N3a** showed a broad peak at 506 nm, whereas the $\lambda_{max}$ of **M3b** appeared at 441 nm at 0 °C, as depicted by broken and dashed–dotted lines in Fig. 8A, respectively.[17] Interestingly, unlike the **Z6a**–**M6b** or **Z3a**–**M3b** case,

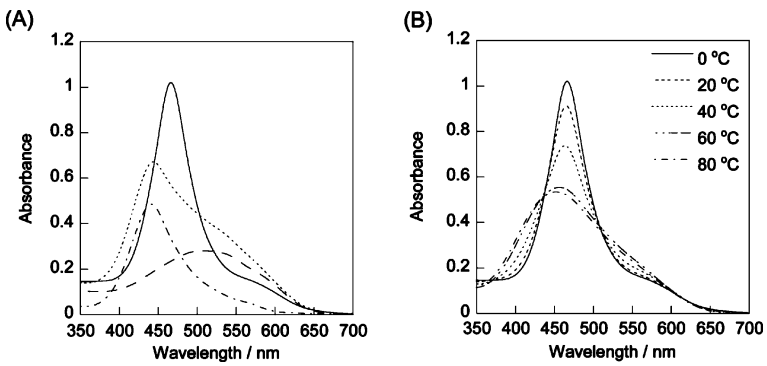


**Fig. 8** (A) UV–Vis spectra of the **N3a**–**M3b** duplex (solid line), single-stranded **N3a** (broken line), **M3b** (dashed–dotted line), and a simple sum of their spectra (dotted line) at 0 °C. (B) UV–Vis spectra of **N3a**–**M3b** at various temperatures. Solution conditions are as follows: [DNA] = 5 μM, [NaCl] = 100 mM, pH 5.0 (10 mM MES buffer).

 

a sharp peak appeared at 466 nm by hybridization of **N3a** with **M3b**. This peak was completely different from the sum of the spectra of single strands that showed broad peaks with a shoulder (compare solid and dotted lines). This sharp peak reversibly broadened above 60 °C where the duplex was dissociated as shown in Fig. 8B. Previously, we have demonstrated that alternate hetero-stacking of Methyl Red and Naphthyl Red allowed merging of each band to a give single peak for the **NS3a**–**MS3b** duplex in which three **N**–**S** and **S**–**M** pairs were introduced alternately.[18] Here, removal of the spacer residue (**S**) from **NS3a**–**MS3b** also induced further hypsochromic shift and narrowing of the band as observed for **MS3a**–**MS3b** and **M3a**–**M3b** (see Fig. S-3 in the ESI†).

**A5a–M5b combination.** Fig. 9 shows the UV–Vis spectra of the **A5a**–**M5b** duplex when changing the temperature from 40 to 0 °C. When the temperature was above 40 °C, a relatively sharp band corresponding to the single-stranded **M5b** was observed. But, a large bathochromic shift as well as broadening of the band was induced at 0 °C where the duplex was formed (note that the $T_m$ of **A5a**–**M5b** was 24.8 °C). Hyperchromicity was also observed concurrently.

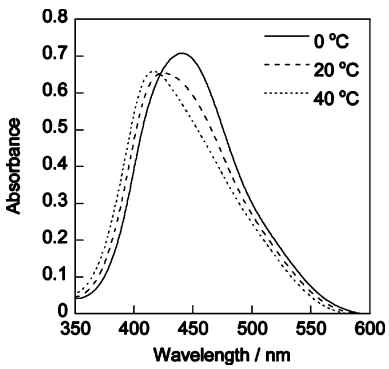


**Fig. 9** UV–Vis spectra of the **A5a**–**M5b** duplex at various temperatures. Solution conditions are as follows: [DNA] = 5 μM, [NaCl] = 100 mM, pH 7.0 (10 mM phosphate buffer).

## Discussion

### 1. Stable "base-pairing" of homo threoninol-nucleotides in the duplex

In the present design, "threoninol-nucleotides", in which functional molecules are tethered on D-threoninols, are introduced at the counterpart of each strand to form a pseudo "base-pair". Such sequence design allowed significant stabilization of the duplex in cases of homo-combination (see Fig. 1A and Table 1). The increase in $T_m$ is derived from the interstrand stacking interaction among the chromophores. But the Methyl Red combination (**M*n*a–M*n*b**) showed an even higher $T_m$ than the azobenzene combination (**Z*n*a–Z*n*b**). This is probably attributed to the stronger dipole–dipole interaction of Methyl Reds because of the push (–$N(CH_3)_2$) and pull (–CONH–) substituents. Such alternate stacking also affected the spectroscopic behavior of the dyes: hybridization of **M3a** and **M3b** induced hypsochromic shift and narrowing of the band with respect to the simple sum of their spectra (Fig. 4). Furthermore, increases in the number of **M** residues caused continuous hypsochromic shift (see Fig. 5A). These shifts are characteristic features of molecular clusters where the molecules are stacked in a face-to-face manner (H-aggregates).[14]

### 2. Stacked structure of the M*n*a–M*n*b duplex

Previously, we have reported that threoninol-nucleotide tethering Methyl Red and 1,3-propanediol (**S** in Scheme 2) were alternately introduced at the center of the DNA sequence, such as **MS3a** and **MS3b**, and the dyes from both strands were stacked with each other. By this sequence design, a molecular cluster was also successfully prepared in the duplex. However, these stacked structures were different from each other as estimated from the UV–Vis and CD spectra. In our previous design involving **S** residues (**MS3a**–**MS3b**), positive and negative CD was strongly induced by hybridization, whereas the present **M3a**–**M3b** duplex did not show such ICD (compare solid line with dotted one in Fig. 6B). Similarly, ICD was rather small up to four **M**–**M** pairs (see Fig. 5B). These ICD demonstrate that Methyl Reds in **MS3a**–**MS3b** formed a right-handed helix resembling natural B-type DNA, and removal of **S** residue (**M3a**–**M3b**) made the helix rewind. In **MS3a**–**MS3b**, winding made the Methyl Reds stack as shown in Fig. 10A because each **M** residue was separated by an **S** residue. But in the absence of **S**, Methyl Reds did not need winding in order to form a firmly stacked structure (Fig. 10B). The threoninol scaffold would allow such a ladder-like structure due to its flexibility.[19] Consequently, the stacking area in **M3a**–**M3b** became larger than that in **MS3a**–**MS3b** and thus **M3a**–**M3b** duplex exhibited a larger hypsochromic shift and narrower band than **MS3a**–**MS3b** due to the stronger exciton coupling (compare solid line with dotted one in Fig. 6A).

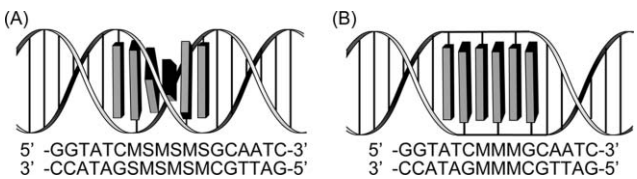


**Fig. 10** Illustration of the possible structure of (A) **MS3a**–**MS3b** duplex involving spacer residue **S** and (B) **M3a**–**M3b** duplex as elucidated from CD spectra.

However, the UV–Vis and CD spectra of **M5a**–**M5b** and **M6a**–**M6b** were different from other **M*n*a–M*n*b** spectra. In particular, **M6a**–**M6b** had stronger ICD with a narrower half-line width (see Fig. 5B and Table 1). Furthermore, the $T_m$ did not increase above $n = 5$, indicating that **M5a**–**M5b** and **M6a**–**M6b** (especially **M6a**–**M6b**) adopted different stacked structures. Since multiplication of dyes caused fairly stable *intramolecular* stacking even in the single-stranded DNA,[20] distal benzene rings of the Methyl Reds from both strands would be partially stacked with each other. Accordingly, the reduced stacked area diminished *intermolecular* stacking and suppressed further stabilization of the duplex.

### 3. Effect of hetero-combinations on the melting temperature and spectroscopic behavior

Hetero combinations such as **Z*n*a–M*n*b** did not destabilize the duplex but raised the $T_m$ with an increase in the number of

threoninol-nucleotides, although the $T_m$ was smaller than that of the corresponding homo combinations. Such an increase in the $T_m$ was associated with the alternate interstrand stacking of the dyes, which also affected the spectroscopic behavior of the Methyl Reds: when **Z6a** was hybridized with **M6b**, broadening and bathochromic shift of the band were observed (Fig. 7). Since the overlapping region of the UV–Vis spectrum between Methyl Red and azobenzene was very small, alternate stacking of Methyl Red and azobenzene disturbed excitonic interaction among the Methyl Red chromophores by the intervening azobenzenes. In contrast, hetero combinations with much wider overlapping absorption (**N3a**–**M3b** combination, see Fig. 8) showed merging of two bands into a single sharp one due to strong exciton coupling among the alternate stacked dyes.[18,21]

Unlike this threoninol-nucleotide combination, hybridization of threoninol-nucleotides with natural ones such as in **A*n*a–M*n*b**, significantly destabilized the duplex as shown in Fig. 1B. This result indicates that dyes on D-threoninol are difficult to stack with molecules on D-ribose.[22] Spectroscopic behavior also reflected a non-stacked structure of Methyl Reds: both bathochromicity and broadening by hybridization of **A5a**–**M5b** were attributable to the disordering of the intrastrand Methyl Reds cluster. In addition, hyperchromism was clearly observed following hybridization. Similar bathochromicity and broadening were also observed for **Z6a**–**M6b**. However, hyperchromicity was not seen because azobenzene and Methyl Reds were firmly stacked. In contrast, hybridization of **A5a** with **M5b** untied the ordered stacking of Methyl Red in the single-stranded **M5b**. Although the number of carbons between the phosphodiester linkage was the same in both cases, the rigid ribose scaffold would be incompatible with flexible D-threoninol.

## Conclusions

(1) Threoninol-nucleotides tethering non-natural functional molecules such as dyes on D-threoninols were consecutively incorporated at the center of an ODN, and an interstrand molecular cluster was successfully prepared by hybridizing them. Clustering of dyes evenly raised the melting temperature due to the stacking interactions.

(2) Interstrand homo-clustering of the dyes (Methyl Reds) exhibited both hypsochromic shift and narrowing of the band, which were characteristic of H-aggregates (H*-aggregates) in which chromophores were vertically stacked. The cluster formed in the duplex was unwound as elucidated from CD spectra.

(3) An alternate hetero cluster was easily prepared by hybridizing two strands involving different threoninol-nucleotides. With a Methyl Red and azobenzene combination (**Z*n*a–M*n*b**), both bathochromicity and broadening of the band were observed due to the disturbance of exciton interactions among Methyl Reds. In contrast, merging of the bands was observed with the Naphthyl Red–Methyl Red combination (**N3a**–**M3b**).

Thus, D-threoninol can be a versatile linker for introducing functional molecules into DNA and stabilizing duplexes. Threoninol-nucleotides facilitate clustering of various functional molecules. With this method, the preparation of highly organized molecular clusters for use as molecular wires or non-linear optical effects is promising.[23]

## Experimental

### Materials

All the conventional phosphoramidite monomers, CPG columns, reagents for DNA synthesis and Poly-Pak II cartridges were purchased from Glen Research. Other reagents for the synthesis of phosphoramidite monomer were purchased from Tokyo Kasei Co., Ltd, and Aldrich.

### Synthesis of the modified DNA involving Methyl Red, Naphthyl Red and azobenzene

All the modified DNAs were synthesized on an automated DNA synthesizer (ABI-3400 DNA synthesizer, Applied Biosystems) by using phosphoramidite monomers bearing dye molecules synthesized according to previous reports,[11a,15a,24] and other conventional ones. Coupling efficiency of the monomers corresponding to modified residues was as high as the conventional ones as judged from the coloration of released trityl cation. After the recommended work-up, they were purified by reversed-phase HPLC and characterized by MALDI-TOFMS (Autoflex II, BRUKER DALTONICS).

MALDI-TOFMS for:

**M1a**: Obsd. 4062 (Calcd. for [**M1a** + $H^+$]: 4063). **M1b**: Obsd. 4065 (Calcd. for [**M1b** + $H^+$]: 4063). **M2a**: Obsd. 4481 (Calcd. for [**M2a** + $H^+$]: 4481). **M2b**: Obsd. 4481 (Calcd. for [**M2b** + $H^+$]: 4481). **M3a**: Obsd. 4899 (Calcd. for [**M3a** + $H^+$]: 4899). **M3b**: Obsd. 4899 (Calcd. for [**M3b** + $H^+$]: 4899). **M4a**: Obsd. 5318 (Calcd. for [**M4a** + $H^+$]: 5317). **M4b**: Obsd. 5317 (Calcd. for [**M4b** + $H^+$]: 5317). **M5a**: Obsd. 5735 (Calcd. for [**M5a** + $H^+$]: 5735). **M5b**: Obsd. 5736 (Calcd. for [**M5b** + $H^+$]: 5735). **M6a**: Obsd. 6155 (Calcd. for [**M6a** + $H^+$]: 6154). **M6b**: Obsd. 6154 (Calcd. for [**M6b** + $H^+$]: 6154). **Z1a**: Obsd. 4020 (Calcd. for [**Z1a** + $H^+$]: 4020). **Z1b**: Obsd. 4019 (Calcd. for [**Z1b** + $H^+$]: 4020). **Z2a**: Obsd. 4395 (Calcd. for [**Z2a** + $H^+$]: 4395). **Z2b**: Obsd. 4396 (Calcd. for [**Z2b** + $H^+$]: 4395). **Z3a**: Obsd. 4770 (Calcd. for [**Z3a** + $H^+$]: 4770). **Z3b**: Obsd. 4771 (Calcd. for [**Z3b** + $H^+$]: 4770). **Z6a**: Obsd. 5898 (Calcd. for [**Z6a** + $H^+$]: 5895). **Z6b**: Obsd. 5898 (Calcd. for [**Z6b** + $H^+$]: 5895). **N3a**: Obsd. 5050 (Calcd. for [**N3a** + $H^+$]: 5049).

### Spectroscopic measurements

The UV–visible and CD spectra were measured on a JASCO model V-550 and a JASCO model J-730, respectively, with a 10 mm quartz cell. Both of them were equipped with programmed temperature-controllers. Conditions of the sample solutions were as follows (unless otherwise noted): [NaCl] = 100 mM, pH 7.0 (10 mM phosphate buffer), [DNA] = 5 μM. For measurements at pH 5.0, 10 mM MES buffer was used.

### Measurement of melting temperature

The melting curve of duplex DNA was obtained with the above apparatus by measuring the change of absorbance at 260 nm *versus* temperature (unless otherwise noted). The melting temperature ($T_m$) was determined from the maximum in the first derivative of the melting curve. Both the heating and cooling curves were measured, and the $T_m$ obtained from them coincided with each other to within 2.0 °C.

## Acknowledgements

This work was supported by Core Research for Evolution Science and Technology (CREST), Japan Science and Technology Agency (JST). Partial supports by a Grant-in-Aid for Scientific Research from the Ministry of Education, Culture, Sports, Science and Technology, Japan and The Mitsubishi Foundation (for H.A.) are also acknowledged.

## References

1 I. Hirao, *Curr. Opin. Chem. Biol.*, 2006, **10**, 622, and references therein.
2 (*a*) J. Kurreck, *Eur. J. Biochem.*, 2003, **270**, 1628; (*b*) C. Wilson and A. D. Keefe, *Curr. Opin. Chem. Biol.*, 2006, **10**, 607.
3 C. Wojczewski, K. Stolze and J. W. Engels, *Synlett*, 1999, 1667.
4 K. Tanaka, A. Tengeiji, T. Kato, N. Toyama and M. Shionoya, *Science*, 2003, **299**, 1212.
5 (*a*) J. Gao, C. Strässler, D. Tahmassebi and E. T. Kool, *J. Am. Chem. Soc.*, 2002, **124**, 11590; (*b*) J. N. Wilson, J. M. Gao and E. T. Kool, *Tetrahedron*, 2007, **63**, 3427.
6 (*a*) M. Kosuge, M. Kubota and A. Ono, *Tetrahedron Lett.*, 2004, **45**, 3945; (*b*) M. Nakamura, Y. Ohtoshi and K. Yamana, *Chem. Commun.*, 2005, **41**, 5163; (*c*) E. Mayer-Enthart and H. A. Wagenknecht, *Angew. Chem., Int. Ed.*, 2006, **45**, 3372; (*d*) V. L. Malinovskii, F. Samain and R. Häner, *Angew. Chem., Int. Ed.*, 2007, **46**, 4464; (*e*) J. Chiba, S. Takeshima, K. Mishima, H. Maeda, Y. Nanai, K. Mizuno and M. Inouye, *Chem.–Eur. J.*, 2007, **13**, 8124.
7 Y. Cho and E. T. Kool, *ChemBioChem*, 2006, **7**, 669.
8 For example: (*a*) K. S. Ramasamy and W. Seifert, *Bioorg. Med. Chem. Lett.*, 1996, **6**, 1799; (*b*) V. S. Rana, V. A. Kumar and K. N. Ganesh, *Bioorg. Med. Chem. Lett.*, 1997, **7**, 2837; (*c*) L. Zhang, A. E. Peritz and E. Meggers, *J. Am. Chem. Soc.*, 2005, **127**, 4174.
9 (*a*) P. S. Nelson, M. Kent and S. Muthini, *Nucleic Acids Res.*, 1992, **20**, 6253; (*b*) K. Yamana, T. Iwai, Y. Ohtani, S. Sato, M. Nakamura and H. Nakano, *Bioconjugate Chem.*, 2002, **13**, 1266; (*c*) U. B. Christensen and E. B. Pedersen, *Nucleic Acids Res.*, 2002, **30**, 4918; (*d*) N. N. Dioubankova, A. D. Malakhov, D. A. Stetsenko, V. A. Korshun and M. J. Gait, *Org. Lett.*, 2002, **4**, 4607; (*e*) A. Okamoto, T. Ichiba and I. Saito, *J. Am. Chem. Soc.*, 2004, **126**, 8364; (*f*) L. L. Zhang and E. Meggers, *J. Am. Chem. Soc.*, 2005, **127**, 74; (*g*) V. Linda and H. A. Wagenknecht, *Synlett*, 2007, **13**, 2111.
10 (*a*) C. F. Stanfield, J. E. Parker and P. Kanellis, *J. Org. Chem.*, 1981, **46**, 4799; (*b*) M. A. Reynolds, T. A. Beck, R. I. Hogrefe, A. McCaffrey, L. J. Arnold and M. M. Vaghefi, *Bioconjugate Chem.*, 1992, **3**, 366; (*c*) K. Fukui, M. Morimoto, H. Segawa, K. Tanaka and T. Shimidzu, *Bioconjugate Chem.*, 1996, **7**, 349; (*d*) A. K. Sharma, P. Kumar and K. C. Gupta, *Helv. Chim. Acta*, 2001, **84**, 3643.
11 (*a*) H. Asanuma, T. Takarada, T. Yoshida, D. Tamaru, X. G. Liang and M. Komiyama, *Angew. Chem., Int. Ed.*, 2001, **40**, 2671; (*b*) X. G. Liang, H. Asanuma, H. Kashida, A. Takasu, T. Sakamoto, G. Kawai and M. Komiyama, *J. Am. Chem. Soc.*, 2003, **125**, 16408.
12 (*a*) C. Brotschi and C. J. Leumann, *Angew. Chem., Int. Ed.*, 2003, **42**, 1655; (*b*) C. Brotschi, G. Mathis and C. J. Leumann, *Chem.–Eur. J.*, 2005, **11**, 1911.
13 Melting temperatures of **A*n*a**–**M*n*b**, **T5a**–**M5b**, **C5a**–**M5b**, and **G5a**–**M5b** are listed in Table S-1 in the ESI.† Absorption maxima and half-line widths of the band of Methyl Red in these duplexes are also shown.
14 (*a*) M. Kasha, *Radiat. Res.*, 1963, **20**, 55; (*b*) K. Norland, A. Ames and T. Taylor, *Photogr. Sci. Eng.*, 1970, **14**, 295.
15 (*a*) H. Asanuma, K. Shirasuka and M. Komiyama, *Chem. Lett.*, 2002, 490; (*b*) H. Kashida, M. Tanaka, S. Baba, T. Sakamoto, G. Kawai, H. Asanuma and M. Komiyama, *Chem.–Eur. J.*, 2006, **12**, 777.
16 Note that **Z6a** did not show either narrowing or hypsochromicity, indicating that azobenzenes were not excitonically interacting.
17 Spectra were measured at pH 5.0 because Naphthyl Red did not show distinct exciton coupling in its deprotonated form. The p$K_a$ of naphthyl red was 6.5 in duplex. Thus, UV–Vis spectra of Naphthyl Red–Methyl Red hetero aggregates were measured at pH 5.0, where Naphthyl Red moieties were protonated. See ref. 18 for effects of pH on the spectroscopic behavior of Naphthyl Red.
18 H. Kashida, H. Asanuma and M. Komiyama, *Angew. Chem., Int. Ed.*, 2004, **43**, 6522.
19 According to Leumann *et al.* (see ref. 12), Bph moieties on D-ribose were partially stacked with each other and adopted a B-DNA conformation from CD measurements, suggesting that multiple Bphs adopted a helical structure. But Methyl Reds on D-threoninol did not adopt such a wound structure as estimated from the small ICD. We think that the flexibility of the threoninol scaffold also contributed to the non-helical structure.
20 The strong CD, especially for **M6a–M6b**, would be derived from the single-stranded **M6a** or **M6b**, in which Methyl Reds adopted a helical structure in the single strand.
21 (*a*) Y. Yonezawa, T. Miyama and H. Ishizawa, *J. Imaging Sci. Technol.*, 1995, **39**, 331; (*b*) R. A. Garoff, E. A. Litzinger, R. E. Connor, I. Fishman and B. A. Armitage, *Langmuir*, 2002, **18**, 6330.
22 The difference in hydrophilicity between the dyes and natural nucleobases may also induce the destabilization of the duplex.
23 (*a*) W. Lin, W. Lin, G. K. Wong and T. J. Marks, *J. Am. Chem. Soc.*, 1996, **118**, 8034; (*b*) O. R. Evans and W. Lin, *Acc. Chem. Res.*, 2002, **35**, 511; (*c*) E. L. Botvinick and J. V. Shah, *Methods Cell Biol.*, 2007, **82**, 81.
24 H. Asanuma, H. Kashida, X. G. Liang and M. Komiyama, *Chem. Commun.*, 2003, 1536.